IOPscience iopscience.iop.org

Home Search Collections Journals About Contact us My IOPscience

Measurement of solid–liquid interfacial energy in the In–Bi eutectic alloy at low melting temperature

This article has been downloaded from IOPscience. Please scroll down to see the full text article.

2007 J. Phys.: Condens. Matter 19 506102

(http://iopscience.iop.org/0953-8984/19/50/506102)

View the table of contents for this issue, or go to the journal homepage for more

Download details:
IP Address: 129.252.86.83
The article was downloaded on 29/05/2010 at 06:57

Please note that terms and conditions apply.

IOP PUBLISHING JOURNAL OF PHYSICS: CONDENSED MATTER

J. Phys.: Condens. Matter **19** (2007) 506102 (16pp) doi:10.1088/0953-8984/19/50/506102

Measurement of solid–liquid interfacial energy in the In–Bi eutectic alloy at low melting temperature

N Maraşlı[1,5], S Akbulut[2], Y Ocak[1,2], K Keşlioğlu[1], U Böyük[2,3], H Kaya[3] and E Çadırlı[4]

[1] Department of Physics, Faculty of Arts and Sciences, Erciyes University, 38039 Kayseri, Turkey
[2] Institute of Science and Technology, Department of Physics, Erciyes University, 38039 Kayseri, Turkey
[3] Department of Science Education, Education Faculty, Erciyes University, 38039 Kayseri, Turkey
[4] Department of Physics, Faculty of Arts and Sciences, Niğde University, Niğde, Turkey

E-mail: marasli@erciyes.edu.tr

Received 10 August 2007, in final form 10 October 2007
Published 8 November 2007
Online at stacks.iop.org/JPhysCM/19/506102

Abstract

The Gibbs–Thomson coefficient and solid–liquid interfacial energy of the solid In solution in equilibrium with In Bi eutectic liquid have been determined to be $(1.46 \pm 0.07) \times 10^{-7}$ K m and $(40.4 \pm 4.0) \times 10^{-3}$ J m^{-2} by observing the equilibrated grain boundary groove shapes. The grain boundary energy of the solid In solution phase has been calculated to be $(79.0 \pm 8.7) \times 10^{-3}$ J m^{-2} by considering force balance at the grain boundary grooves. The thermal conductivities of the In–12.4 at.% Bi eutectic liquid phase and the solid In solution phase and their ratio at the eutectic melting temperature (72 °C) have also been measured with radial heat flow apparatus and Bridgman-type growth apparatus.

1. Introduction

The solid–liquid interfacial energy, σ_{SL}, is recognized to play a key role in a wide range of metallurgical and materials phenomena, from wetting [1] and sintering through to phase transformations and coarsening [2]. Thus, a quantitative knowledge of σ_{SL} values is necessary. However, the determination of σ_{SL} is more difficult. The earliest direct determinations were derived from droplet undercooling measurements, on the supposition that maximum observed undercooling signified homogeneous nucleation. An empirical relationship between the interfacial energy and the melting enthalpy change to estimate the interfacial energy was proposed by Turnbull [3] and is expressed as

$$\sigma_{SL} = \frac{\tau \Delta H_M}{V_S^{2/3} N_a^{1/3}}, \tag{1}$$

[5] Author to whom any correspondence should be addressed.

 © 2007 IOP Publishing Ltd Printed in the UK

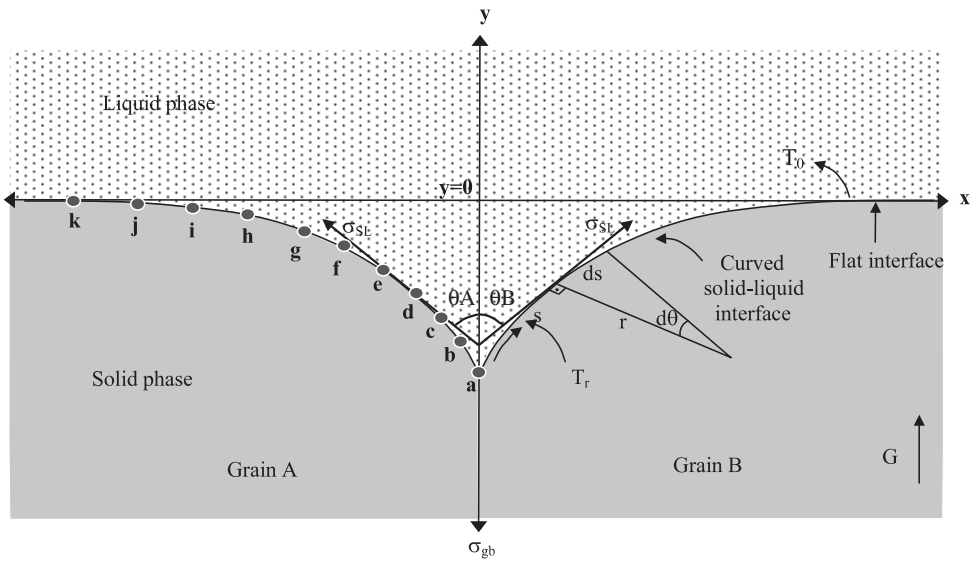

Figure 1. Schematic illustration of an equilibrated grain boundary groove formed at a solid–liquid interface in a temperature gradient showing the definitions of r, θ.

where the coefficient τ was found to be 0.45 for metals and 0.34 for nonmetallic systems [3], ΔH_{M} is the enthalpy change of fusion, V_{S} is the molar volume of the solid phase and N_{a} is the Avogadro constant. However, the experiments generated substantially large values of undercooling, resulting in large values of σ_{SL}, indicating that such experiments typically underestimate σ_{SL}, except where there is independent evidence that homogeneous rather than heterogeneous nucleation was operative. Other disadvantages of deriving σ_{SL} from undercooling experiments were discussed by Jones [4] and Eustathopoulos [5].

A technique for the quantification of the interfacial free energy from the solid–liquid interfacial grain boundary groove shape has been established. This technique is based on direct application of the Gibbs–Thomson equation and can be applied to measure σ_{SL} for multi-component systems as well as pure materials, for opaque materials as well as transparent materials, for any observed grain boundary groove shape, and for any $R = K_{\mathrm{L}}/K_{\mathrm{S}}$ value. When the solid–liquid interface is equilibrated with a grain boundary in a temperature gradient, the shape of a grain boundary groove is formed by the intersection of planar grain boundaries with an otherwise planar solid–liquid interface, as shown in figure 1. At the equilibrium conditions, the curvature undercooling, ΔT_r, is the temperature difference between the temperature of a flat interface (T_0) and the temperature of a curved interface (T_r). When the solid–liquid interfacial free energy is isotropic, the curvature undercooling is given by the following equation for the case of a planar grain boundary intersecting a planar solid–liquid interface:

$$\Gamma = r\Delta T_r = \frac{T_{\mathrm{E}} V_{\mathrm{S}} \sigma_{\mathrm{SL}}}{\Delta H_{\mathrm{M}}} = \frac{\sigma_{\mathrm{SL}}}{\Delta S_{\mathrm{f}}}, \tag{2}$$

where Γ is the Gibbs–Thomson coefficient, T_{E} is the equilibrium temperature or melting temperature, V_{S} is the molar volume of solid, ΔH_{M} is the enthalpy change, ΔS_{f} is the entropy change of fusion per unit volume, and r is the radius of the groove profile, as shown in figure 1. This equation is called the Gibbs–Thomson equation for a curved interface having an isotropic solid–liquid interfacial energy, and is useful for considering the effect of the solid–liquid interfacial energy on solidification and melting, as it expresses the effective change in melting point for a curved interface.

Equation (2) may be integrated in the y direction (perpendicular to the macroscopic interface) from the flat interface to a point on the cusp, as shown in figure 1:

$$\int_0^{-y} \Delta T_r \, \mathrm{d}y = \Gamma \int_0^{-y} \frac{1}{r} \, \mathrm{d}y. \tag{3}$$

The right-hand side of equation (3) may be evaluated for any shape by noting that, by definition, $\mathrm{d}s = r \, \mathrm{d}\theta$ and $\mathrm{d}y = r \cos\theta \, \mathrm{d}\theta$ (s and θ are shown in figure 1) so that

$$\Gamma \int_0^{-y} \frac{1}{r} \, \mathrm{d}y = -\Gamma \int_0^{y} \frac{1}{r} \, \mathrm{d}y = -\Gamma \int_{\pi/2}^{\theta} \frac{1}{r} r \cos\theta \, \mathrm{d}\theta = \Gamma(1 - \sin\theta). \tag{4}$$

The left-hand side of equation (3) may be evaluated if ΔT_r is known as a function of y. When the thermal conductivities of solid and liquid phases are equal, the temperature depends just on temperature gradient and the distance, that is:

$$\Delta T_r = Gy \tag{5}$$

so that

$$\tfrac{1}{2} G y^2 = \Gamma(1 - \sin\theta). \tag{6}$$

The value of Γ may be obtained from the slope of a plot of y^2 against $(1 - \sin\theta)$. The theoretical basis of the grain boundary groove profile method was given by Bolling and Tiller [6] for equal thermal conductivities of solid and liquid phases, and the first report of its application to measure σ_{SL} was by Jones and Chadwick [7] for some transparent materials. Nash and Glicksman [8] extended Bolling and Tiller's analysis to include the effects of unequal thermal conductivities of solid and liquid phases. Measurements of solid–liquid interfacial energies were made for some transparent organic materials [3–14].

The technique was extended to measure σ_{SL} for alloys by Gündüz and Hunt [15, 16]. The observation of the grain boundary groove shape in an alloy is obviously very difficult. Gündüz and Hunt [15] have developed an apparatus to obtain the grain boundary groove shape in binary eutectic systems. The details of the apparatus and experimental procedures are given in [15]. Gündüz and Hunt [15] also developed a finite difference model to calculate the corresponding difference in temperature, ΔT_r, between the flat interface for each point on the grain boundary groove shapes and evaluated the right-hand side of the equation (3) by measuring the values of θ. The values of θ were obtained by fitting a Taylor expansion to the adjacent points on the cusp. Usually the points from **b** to **i** shown in figure 1 were used to obtain more reliable Γ values with Gündüz and Hunt's model. This numerical method calculates the temperature along the interface of a measured grain boundary groove shape rather than attempting to predict the equilibrium grain boundary groove shape. If the grain boundary groove shape, the temperature gradient in the solid, G_{S}, and the ratio of thermal conductivity of the equilibrated liquid phase to solid phase, $R = K_{\mathrm{L}}/K_{\mathrm{S}}$, are known or measured, then the value of the Gibbs–Thomson coefficient is obtained with the Gündüz and Hunt numerical method. Measurements of the solid–liquid interface energies were made in metallic binary eutectic based systems [15–20].

Bayender *et al* [21] modified the apparatus originally designed by Hunt *et al* [22] to observe the equilibrated grain boundary groove shape directly for transparent materials. They applied Gündüz and Hunt's numerical method to determine the Gibbs–Thomson coefficients, solid–liquid interface energies and grain boundary energies. Measurements of the solid–liquid interface energies were made in transparent organic binary systems [23–26].

Indium has been used widely in soldering, the aeroplane industry and other types of industry. Until now, the measurements of solid–liquid interfacial energies in metallic binary alloys were made at above the 140 °C melting temperature, and were not made at lower than the 100 °C equilibrating temperature because of the difficulty of temperature control on the

sample and worries about quenching of the interface at the low equilibrating temperature. Thus the aims of the present work were to observe the grain boundary groove shapes in metallic alloys at the low equilibrating temperature and to determine the Gibbs–Thomson coefficient, solid–liquid interfacial energy and grain boundary energy for solid In solution (In–12.4 at.% Bi) in equilibrium with In–22 at.% Bi eutectic liquid from the observed grain boundary groove shapes.

2. Experimental procedure

2.1. Experimental apparatus

To observe the equilibrated grain boundary groove shapes in opaque materials, Gündüz and Hunt [15, 16] designed a radial heat flow apparatus. Maraşlı and Hunt [17] improved the experimental apparatus for higher temperatures. The details of the apparatus and experimental procedures are given in [15–17]. In the experimental technique, the sample was heated from the centre by a single heating wire and the outside of the sample was kept cool by water cooling to get a constant radial temperature gradient in the sample. A thin liquid layer was melted around the central heating wire and annealed for a long enough period in a constant radial temperature gradient. At the end of the annealing period, the sample was quenched by just cutting off the power. Cooling of the sample from the outside must be more effective to get a well-quenched solid–liquid interface. Water cooling was sufficient to get a well-defined solid–liquid interface at the high equilibrating temperature, but after a few experimental works it was seen that water cooling was insufficient to obtain a well-defined solid–liquid interface at the lower equilibrating temperature which is smaller than 100 °C. The melting point of In–22 at.% Bi eutectic alloy is 72 °C. Thus, the outside of sample was kept at −10 °C using a *Poly Science digital 9102* model heating/refrigerating circulating bath containing an aqueous ethylene glycol solution, and the gap between the cooling jacket and the sample was filled with graphite dust to get a well-quenched solid–liquid interface in the present work. The temperature of the circulating bath was kept constant at −10 °C to an accuracy of ±0.01 °C and the temperature on the sample was controlled to an accuracy of ±0.01 °C with a *Eurotherm 2604*-type controller.

2.2. Sample production

Consider a binary eutectic system. Above the eutectic temperature, a binary eutectic system consists of solid and liquid provided that the alloy compositions $C_\alpha < C_0 < C_E$ or $C_E > C_0 < C_\beta$, where C_E, C_α, and C_β are the composition of the eutectic, solid α and solid β phases, respectively. If this eutectic system is held in a very stable temperature gradient, the liquid droplets move up the temperature gradient by temperature gradient zone melting (TGZM) and single solid can grow on the eutectic structure during the annealing period. When the composition of the alloy is far from the eutectic composition, the experiment usually needs a long time to reach equilibrium due to the larger freezing range. If the alloy composition is near the eutectic composition, above the eutectic temperature, a binary eutectic system consists of liquid. If this system is held in a very stable temperature gradient, there will be no liquid droplets behind the solid phase and two solid phases can grow together on the eutectic structure. The equilibrating time for this system should be shorter because of the small freezing range.

The maximum solubility of bismuth in indium is about 12.4 at.% Bi at the eutectic melting temperature, which is 72 °C [27]. Thus the composition of alloy was chosen to be In–12.4 at.% Bi to growth the single solid In solution phase from the eutectic liquid on the eutectic structures. In–12.4 at.% Bi alloy was prepared in a vacuum furnace by using 99.99% pure indium and

99.9% pure bismuth. After stirring, the molten alloy was poured into a graphite crucible held in a specially constructed casting furnace at approximately 30 K above the melting point of the alloy. The molten metal was then directionally frozen from the bottom to the top to ensure that the crucible was completely full. The sample was then placed in the radial heat flow apparatus.

The experiments were carried out in two steps. In the first step, the thermocouples were calibrated by detecting the melting point during very slow heating and cooling using a lower temperature gradient operational mode. In the second step, the specimen was heated from the centre using a single heating wire (1.7 mm in diameter, Kanthal A-1) and the outside of the specimen was kept at $-10\,^{\circ}$C using a *Poly Science digital 9102* model heating/refrigerating circulating bath containing an aqueous ethylene glycol solution. A thin liquid layer (1–2 mm thick) was melted around the central heater and the specimen was annealed in a very stable temperature gradient for a long time. The annealing time for In–12.4 at.% Bi alloy was 4 days. During the annealing period, the temperature in the specimen and the vertical temperature variations on the sample were recorded continuously by the stationary thermocouples and a movable thermocouple, respectively, using a data logger via computer, and the input power was recorded periodically. The temperature in the sample was stable to about ± 0.025 K for hours and ± 0.05 K for up to 4 days. At the end of the annealing time the specimen was rapidly quenched by turning off the input power, which is sufficient to get a well-defined solid–liquid interface, because the liquid layer around the central heating wire was very thin (typically less than 0.5–1 mm).

2.3. Measurements of the coordinates of equilibrated grain boundary groove shapes

The quenched sample was cut transversely into lengths of typically 25 mm, and transverse sections were ground flat with 180 grit SiC paper. Grinding and polishing were then carried out by following a standard route. After polishing, the samples were etched with a 4 g picric acid ($(NO_2)_3C_6H_2OH$) and 20 ml of hydrochloric acid (HCl) in 400 ml of ethanol (C_2H_5OH) for 3 s.

The equilibrated grain boundary groove shapes were then photographed with a *Honeywell CCD* digital camera placed in conjunction with an *Olympus BH2* type light optical microscope. A graticule ($200 \times 0.01 = 2$ mm) was also photographed using the same objective. The photographs of the equilibrated grain boundary groove shapes and the graticule were superimposed on one another using *Adobe PhotoShop 8.0* version software, so that accurate measurements of the groove coordinate points on the groove shapes could be made.

2.4. Geometrical correction for the groove coordinates

The coordinates of the cusp, x, y, should be measured using the coordinates x, y, z, where the x axis is parallel to the solid–liquid interface, the y axis is normal to the solid–liquid interface, and the z axis lies at the base of the grain boundary groove, as shown in figure 2(a). The coordinates of the cusp x', y' from the metallographic section must be transformed to x, y coordinates. Maraşlı and Hunt [17] devised a geometrical method to make appropriate corrections to the groove shapes, and the details of the geometrical method are given in [17].

The relation between x and x' can be expressed as [17]

$$\begin{aligned} x &= x' \cos\alpha \\ x &= x' \frac{\sqrt{a^2 + d^2}}{\sqrt{a^2 + b^2 + d^2}} \end{aligned} \tag{7}$$

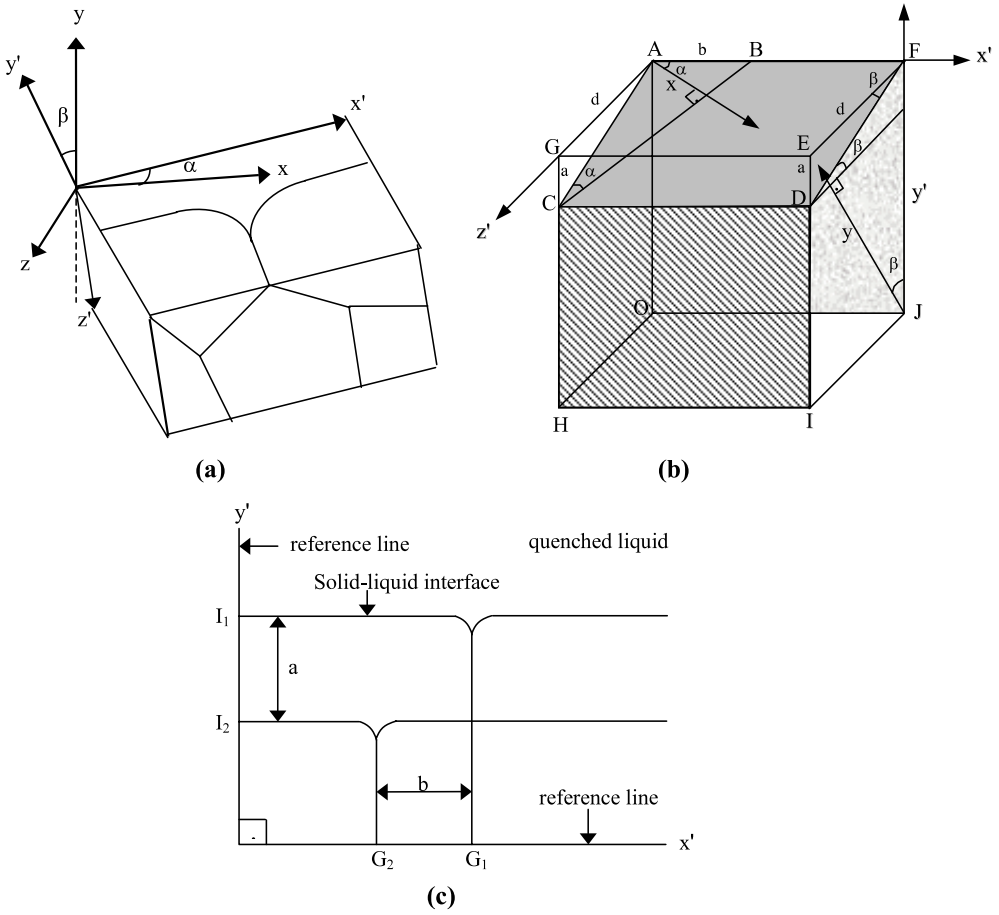

Figure 2. (a) Schematic illustration of the relationship between the actual coordinates, x, y, and the measured coordinates, x', y', of the groove shape; (b) schematic illustration for the metallic examination of the sample, where B is the location of the grain boundary groove shape onto the first plane OJFA, C is the location of the grain boundary groove shape onto the second plane HIDC, AB $= b$, CG $=$ ED $= a$ and AG $= d$; (c) schematic illustration of the displacement of the grain boundary groove shape position along the x' and y' axes [17].

and the relation between y and y' can be expressed as [17]

$$y = y' \cos \beta$$
$$y = y' \frac{d}{\sqrt{a^2 + d^2}}, \tag{8}$$

where d is the distance between the first and second planes along the z' axis, b is the displacement of the grain boundary position along the x' axis, a is the displacement of the solid–liquid interface along the y' axis, α is the angle between the x' axis and the x axis, and β is the angle between the y' axis and the y axis, as shown in figure 2. In this work, the values of a, b and d were measured in order to transform the cusps coordinates x', y' into the x, y coordinates as follows.

Two perpendicular reference lines (approximately 0.1 mm thick and 0.1 mm deep) were marked near the grain boundary groove on the polished surface of the sample (figure 2(c)). The samples were then polished and the grain boundary groove shapes were photographed.

The thickness of the sample d_1 was measured using a digital micrometer (with a resolution of 1 μm) at several points of the sample to obtain the average value. After thickness measurements had been made, the sample was again polished to remove a thin layer (at least 40–50 μm) from the sample surface. The same grain boundary groove shapes were again photographed and the thickness of the sample, d_2, was measured with the same micrometer. The difference in the thickness of the sample, $d = d_1 - d_2$, gave the layer removed from the sample surface. The photographs of the grain boundary groove shapes were superimposed on each other using *Adobe PhotoShop 8.0* version software to measure the displacement of the solid–liquid interface along the y' axis and the displacement of the grain boundary groove position along the x' axis (see figure 2(b)). Thus the required a, b and d measurements were made so that appropriate corrections to the shape of the grooves could be deduced [17].

The coordinates of equilibrated grain boundary groove shapes were measured with an optical microscope to an accuracy of ± 10 μm. The thickness of the sample (2–2.5 cm long) for geometrical correction was measured using a digital micrometer with ± 1 μm resolution. Thus the uncertainty in the measurements of equilibrated grain boundary coordinates was less than 0.2%.

2.5. Thermal conductivities of the solid and liquid phases

The thermal conductivity ratio of the In–22 at.% Bi eutectic liquid phase to the solid In solution phase (In–12.4 at.% Bi), $R = K_{\mathrm{L(eutectic\ liquid)}}/K_{\mathrm{S(solid\ In\ solution)}}$, must be known or measured to evaluate the Gibbs–Thomson coefficients using the present numerical method. The radial heat flow apparatus is an ideal technique for measuring the thermal conductivity of the solid phases. The thermal conductivity of solid In solution (In–12.4 at.% Bi) is needed to evaluate the temperature gradient on the solid phase. In the radial heat flow method, a cylindrical sample was heated by using a single heating wire along the axis at the centre of the sample, and the sample was kept in a very stable temperature gradient for a period to achieve steady-state conditions. At the steady-state condition, the temperature gradients in the cylindrical specimen are given by Fourier's law,

$$\frac{\mathrm{d}T}{\mathrm{d}r} = -\frac{Q}{AK_{\mathrm{S}}}, \tag{9}$$

where Q is the total input power from the centre of the specimen, A is the surface area of the specimen and K_{S} is the thermal conductivity of the solid phase. Integration of equation (9) gives

$$K_{\mathrm{S}} = \frac{1}{2\pi\ell}\ln\left(\frac{r_2}{r_1}\right)\frac{Q}{T_1 - T_2} \tag{10}$$

$$K_{\mathrm{S}} = a_0\frac{Q}{T_1 - T_2}, \tag{11}$$

where $a_0 = \ln(r_2/r_1)/2\pi\ell$ is an experimental constant, r_1 and $r_2 (r_2 > r_1)$ are fixed distances from the centre axis of the specimen, ℓ is the length of the heating wire (which is constant) and T_1 and T_2 are the temperatures at the fixed positions r_1 and r_2 from the centre axis of the specimen. Equation (11) could be used to obtain the thermal conductivity of the solid phase by measuring the difference in temperature between the two fixed points for a given power level, provided that the vertical temperature variation is a minimum or zero.

The thermal conductivity of the solid In solution (In–12.4 at.% Bi) was measured in the radial heat flow apparatus. The alloy was prepared in a vacuum furnace by using 99.99% purity indium and 99.9% purity bismuth. The sample was heated using the central heating wire in steps of 10 K, from 313.2 K up to 5 K below the eutectic temperature (345.3 K). The

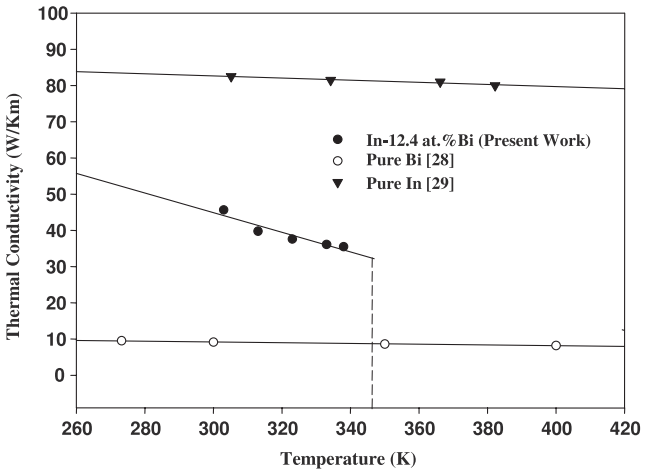

Figure 3. Thermal conductivity of solid indium solution versus temperature.

Table 1. Thermal conductivities of solid and liquid phases and their ratios at their melting temperatures for the In–Bi binary eutectic system.

Alloy	Phases	Melting temperature (K)	K (W K^{-1} m^{-1})	$R = K_L/K_S$
In–Bi	Solid In solution (In–12.4 at.% Bi)	345.15	32.82	0.84
	Eutectic liquid (In–22 at.% Bi)	345.15	27.56	

samples were kept at steady state for at least 2 h. At the steady-state condition, the total input power, vertical temperature variations on the sample and the temperatures in the sample were measured. When all desired power and temperature measurements had been completed, the sample was left to cool down to room temperature.

The thermal conductivities of solid In solution (In–12.4 at.% Bi) versus temperature are shown in figure 3. The value of K_S for the solid In solution at the eutectic melting temperature was obtained as 32.82 W K^{-1} m^{-1} by extrapolating to the eutectic temperature, as shown in figure 3. The values of thermal conductivities used in the calculations are given in table 1.

It is not possible to measure the thermal conductivity of the liquid phase with the radial heat flow apparatus, since a thick liquid layer (10 mm) is required. A layer of this size would certainly have led to convection. If the thermal conductivity ratio of the liquid phase to the solid phase is known and the thermal conductivity of the solid phase is measured at the melting temperature, the thermal conductivity of the liquid phase can then be evaluated. The thermal conductivity ratio can be obtained during directional growth with a Bridgman-type growth apparatus. The heat flow away from the interface through the solid phase must balance that liquid phase plus the latent heat generated at the interface, i.e. [30]

$$VL = K_S G_S - K_L G_L, \tag{12}$$

where V is the growth rate, L is the latent heat, G_S and G_L are the temperature gradients in the solid and liquid, respectively, and K_S and K_L are the thermal conductivities of the solid and liquid phases, respectively. For very low velocities, $VL \ll K_S G_S$, so that the conductivity

ratio, R, is given by

$$R = \frac{K_{\mathrm{L}}}{K_{\mathrm{S}}} = \frac{G_{\mathrm{S}}}{G_{\mathrm{L}}}. \tag{13}$$

A directional growth apparatus, firstly constructed by McCartney [31], was used to find out the thermal conductivity ratio, $R = K_{\mathrm{L}}/K_{\mathrm{S}}$. A thin-walled graphite crucible, 6.3 mm OD × 4 mm ID × 180 mm in length, was used to minimize convection in the liquid phase.

Molten In–12.4 at.% Bi alloy was poured into the thin-walled graphite tube and the molten alloy was then directionally frozen from bottom to top to ensure that the crucible was completely full. The specimen was then placed in the directional growth apparatus. The specimen was heated to 30 K over the melting temperature of the alloy. The specimen was then left to reach thermal equilibrium for at least 2 hours. The temperature in the specimen was measured with an insulated K-type thermocouple. In the present work, a 1.2 mm OD × 0.8 mm ID alumina tube was used to insulate the thermocouple from the melt, and the thermocouple was placed perpendicular to the heat flow (growth) direction. At the end of equilibration, the temperature in the specimen was stable to ±0.5 K for a short-term period and to ±1 K for a long-term period. When the specimen temperature stabilized, the directional growth was started by turning the motor on. The cooling rate was recorded with a data logger via computer. In the present measurements, the growth rate was 8.3×10^{-4} cm s^{-1}. When the solid–liquid interface passed the thermocouple, a change in the slope of the cooling rate for liquid and solid phases was observed. When the thermocouple reading was approximately 30 K below the melting temperature, the growth was stopped by turning the motor off.

The thermal conductivity ratio can be evaluated from the ratio of cooling rates for the liquid phase and the solid phase. The cooling rate of the liquid and solid phases is given by

$$\left(\frac{\mathrm{d}T}{\mathrm{d}t}\right)_{\mathrm{L}} = \left(\frac{\mathrm{d}T}{\mathrm{d}x}\right)_{\mathrm{L}}\left(\frac{\mathrm{d}x}{\mathrm{d}t}\right)_{\mathrm{L}} = G_{\mathrm{L}}V \tag{14}$$

and

$$\left(\frac{\mathrm{d}T}{\mathrm{d}t}\right)_{\mathrm{S}} = \left(\frac{\mathrm{d}T}{\mathrm{d}x}\right)_{\mathrm{S}}\left(\frac{\mathrm{d}x}{\mathrm{d}t}\right)_{\mathrm{S}} = G_{\mathrm{S}}V. \tag{15}$$

From equations (13), (14) and (15), the thermal conductivity ratio can be written as

$$R = \frac{K_{\mathrm{L}}}{K_{\mathrm{S}}} = \frac{G_{\mathrm{S}}}{G_{\mathrm{L}}} = \frac{(\frac{\mathrm{d}T}{\mathrm{d}t})_{\mathrm{S}}}{(\frac{\mathrm{d}T}{\mathrm{d}t})_{\mathrm{L}}}, \tag{16}$$

where the $(\mathrm{d}T/\mathrm{d}t)_{\mathrm{S}}$ and $(\mathrm{d}T/\mathrm{d}t)_{\mathrm{L}}$ values were directly measured from the temperature versus time curve shown in figure 4. The ratio of the thermal conductivity of the eutectic liquid (In–22 at.% Bi) to the solid In solution (In–12.4 at.% Bi), $R = K_{\mathrm{L(eutectic)}}/K_{\mathrm{S(In\ solution)}}$ was found to be 0.84, as shown in figure 4. The values of K_{L} and K_{S} used in the determination of the Gibbs–Thomson coefficients are also given in table 1.

The estimated experimental error in the measurement of K_{S} is the sum of the fractional uncertainty of the measurements of power, temperature differences, length of heating wire and thermocouple positions, which can be expressed as

$$\left|\frac{\Delta K_{\mathrm{S}}}{K_{\mathrm{S}}}\right| = \left|\frac{\Delta Q}{Q}\right| + \left|\frac{\Delta T_1}{T_1}\right| + \left|\frac{\Delta T_2}{T_2}\right| + \left|\frac{\Delta \ell}{\ell}\right| + \left|\frac{\Delta r_1}{r_1}\right| + \left|\frac{\Delta r_2}{r_2}\right|. \tag{17}$$

The estimated error in the thermal conductivity measurements is about 5% [32].

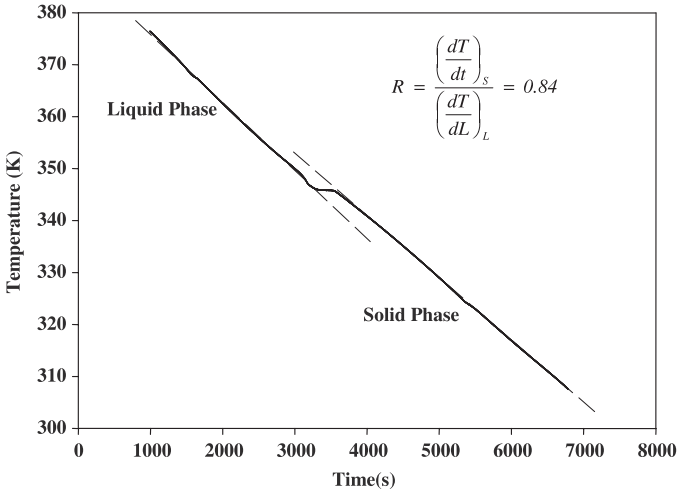

Figure 4. Cooling rate of In–12.4 at.% Bi alloy.

2.6. Temperature gradient measurement in the solid phase

The cylindrical sample was heated from the centre by a thin heating wire and a thin liquid layer was melted around the central heating element. At steady state, the temperature gradient at radius r is given by

$$G_S = \frac{dT}{dr} = -\frac{Q}{2\pi r \ell K_S}, \tag{18}$$

where Q is the input power, ℓ is the length of the heating element, r is the distance of the solid–liquid interface to the centre of the sample, and K_S is the thermal conductivity of the solid phase.

The average temperature gradient of the solid phase must be determined for each grain boundary groove shape. This was done by measuring the input power, the length of the heating element and the position of the solid–liquid interface and the value of K_S for the solid In solution (In–12.4 at.% Bi) at the eutectic melting point. By using these measured values in equation (18), the temperature gradient can be determined for each grain boundary groove shape.

The estimated experimental error in the measurement of temperature gradient is a sum of the fractional uncertainty in the measurements of power, the length of the heating wire, the thermal conductivity and the thermocouples' positions, which can be expressed as

$$\left|\frac{\Delta G_S}{G_S}\right| = \left|\frac{\Delta Q}{Q}\right| + \left|\frac{\Delta \ell}{\ell}\right| + \left|\frac{\Delta r}{r}\right| + \left|\frac{\Delta K_S}{K_S}\right|. \tag{19}$$

If equation (19) is compared with equation (17), the experimental errors came from the measurements of Q, ℓ, r in equation (19), which already exist in the fractional uncertainties at the equation (17). Thus the total experimental error in the thermal gradient measurements is equal to the experimental error in thermal conductivity measurements, and is about 5%.

Table 2. The values of the Gibbs–Thomson coefficient for solid In solution (In–12.4 at.% Bi) in equilibrium with In–22 at.% Bi eutectic liquid, as determined in the present work. The subscripts LHS and RHS refer to the left-hand side and the right-hand side of the groove, respectively.

				Gibbs–Thomson coefficient	
Groove no	$G_K \times 10^2$ (K m^{-1})	α (deg)	β (deg)	$\Gamma_{\mathrm{LHS}} \times 10^{-7}$ (K m)	$\Gamma_{\mathrm{RHS}} \times 10^{-7}$ (K m)
a	17.29	19.6	11.8	1.44	1.46
b	17.48	16.7	12.0	1.48	1.43
c	17.84	20.9	23.5	1.50	1.48
d	17.95	8.9	8.1	1.49	1.50
e	18.16	6.3	8.5	1.47	1.45
f	20.69	5.7	10.6	1.43	1.44
g	18.05	7.3	13.1	1.47	1.46
h	16.14	19.4	10.9	1.49	1.44
i	21.64	18.0	17.1	1.47	1.40
j	18.83	10.9	9.2	1.48	1.43
				$\bar{\Gamma} = (1.46 \pm 0.07) \times 10^{-7}$ K m	

3. Results and discussion

3.1. Determination of Gibbs–Thomson coefficient

If the thermal conductivity ratio of the liquid phase to the solid phase, the coordinates of the grain boundary groove shapes and the temperature gradient of the solid phase are known, then the Gibbs–Thomson coefficient (Γ) can be obtained by using the numerical method described in detail [15]. The experimental error in the determination of the Gibbs–Thomson coefficient is the sum of the experimental errors in the measurements of the temperature gradient, thermal conductivity and groove coordinates. Thus the total error in the determination of the Gibbs–Thomson coefficient is about 5%.

In the present work, the Gibbs–Thomson coefficients for the solid In solution (In–12.4 at.% Bi) in equilibrium with In–22 at.% Bi eutectic liquid were determined with the present numerical model by using ten equilibrated grain boundary groove shapes. The grooves examined in this system are shown in figure 5. As can be seen from figure 5, a very thin In_2B_i (In–33.2 at.% Bi) layer which is smaller then 1 μm formed in front of the solid In solution phase (In–12 at.% Bi), and this allows a well-defined solid–liquid interface to be observed during the quench, and also the phases, grains and interfaces of the system are very clear. The values of Γ for solid In solution (In–12 at.% Bi) are given in table 2. The average value of Γ from table 2 is $(1.46 \pm 0.07) \times 10^{-7}$ K m for solid In solution (In–12.4 at.% Bi) in equilibrium with In–22 at.% Bi eutectic liquid.

3.2. Determination of entropy of fusion per unit volume

It is also necessary to know the entropy of fusion per unit volume, ΔS_f, for the determination of the solid–liquid interfacial energy. For pure materials the entropy of fusion per unit volume is given by

$$\Delta S_f^* = \frac{\Delta H_{\mathrm{M}}}{T_{\mathrm{M}}} \frac{1}{V_{\mathrm{S}}}, \tag{20}$$

where ΔH_{M} is the enthalpy change in the solid phase at the melting temperature, T_{M} is the melting temperature, and V_{S} is the molar volume of the solid phase. If the solid phase is

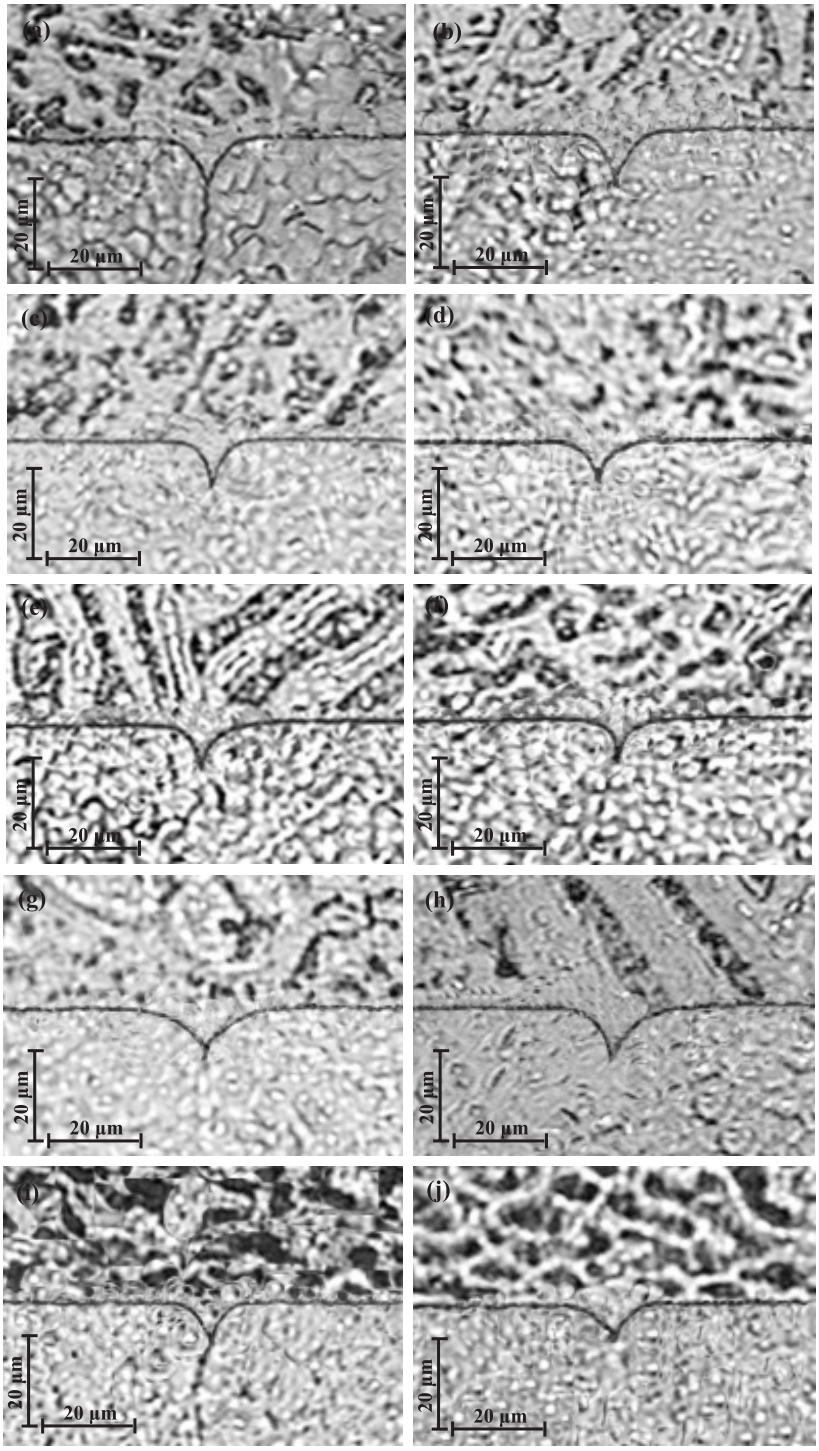

Figure 5. Typical grain boundary groove shapes for solid In solution in equilibrium with In–22 at.% Bi eutectic liquid.

Table 3. Some physical properties of solid In solution (In–12.4 at.% Bi) phase at the eutectic temperature.

System	In–Bi eutectic
Composition of the quenched liquid phase, C_L	In–22 at.% Bi [27]
Composition of solid In solution phase, C_S	In–12.4 at.% Bi [27]
$f(C)$[a]	−0.56 [27]
Eutectic melting temperature, T_m (K)	345.15 [27]
Molar volume of solid In, V_{In} (m^3)	15.75×10^{-6} [33]
Molar volume of solid Bi, V_{Bi} (m^3)	21.31×10^{-6} [33]
Molar volume of solid In solution (In–12.4 at.% Bi), $V_{(In-12.4\ at.\%\ Bi)}$, (m^3)	13.10×10^{-6}
Liquidus slope, m_L (K/at.fr)	−440.4 [27]
Entropy change of fusion, ΔS_f (J K^{-1} m^{-3})	2.77×10^5

[a] $f(C) = \frac{C_S - C_L}{(1-C_L)\,C_L}$.

solid solution, then the molar volume of the solid is replaced by the molar volume of the solid solution. The molar volume of solid solution is given by [33],

$$V_{SS} = V_S - \sum_i x_i V_i^*, \tag{21}$$

where V_{SS} is the molar volume of solid solution, x_i is the molar fraction of the ith metal and V_i^* is the molar volume of ith metal in the pure state. The change in entropy for an alloy is given by [15],

$$\Delta S_f = \frac{(1 - C_S)(S_A^L - S_A^S) + C_S(S_B^L - S_B^S)}{V_S}, \tag{22}$$

where S_A^L, S_A^S, S_B^L and S_B^S are partial molar entropies for A and B materials and C_S is the solid composition. Since the entropy terms are generally not available, for convenience, the undercooling at constant composition may be related to the change in composition at constant temperature. For a sphere [34]

$$\Delta C_r = \frac{2\sigma_{SL} V_S (1 - C_L) C_L}{r R T_M (C_S - C_L)}, \tag{23}$$

where R is the gas constant. For small changes

$$\Delta T_r = m_L \Delta C_r = \frac{2 m_L \sigma_{SL} V_S (1 - C_L) C_L}{r R T_M (C_S - C_L)}. \tag{24}$$

For a spherical solid, $r_1 = r_2 = r$ and the curvature undercooling is written by

$$\Delta T_r = \frac{2\sigma_{SL}}{r \Delta S_f}. \tag{25}$$

From equation (24) and (25), the entropy change for an alloy is written as

$$\Delta S_f = \frac{R T_M}{m_L V_S} \frac{C_S - C_L}{(1 - C_L) C_L}. \tag{26}$$

The values of the relevant constant obtained from [27] and the calculated entropy change of fusion per unit volume are given in table 3. The error in the determination of entropy change of fusion per unit volume is estimated to be about 5% [35].

Table 4. A comparison of the solid–liquid interface energy measured in the present work with values obtained in previous works. (Note: CNE—classical nucleation experiments; GBG—grain boundary groove method.)

				Solid–liquid interface energy $\sigma_{SL} \times 10^{-3}$ (J m^{-2})	
System	Solid phase	Liquid phase	Temperature (K)	Theoretical	Experimental
In	In	In	430.15	34 [36] 48 [38] 34 [40]	30.8 [37] CNE 36.0 [39] CNE
In–Bi	In solution (In–12.4 at.% Bi)	Eutectic liquid (In–22 at.% Bi)	345.15	—	40.4 ± 4.0 GBG (present work)

3.3. Evaluation of solid–liquid interfacial energy

If the values of Γ and ΔS_f are known, the value of solid–liquid interfacial energy, σ_{SL} can be evaluated from equation (2). The solid–liquid interfacial energy of the solid In solution phase (In–12.4 at.% Bi) in equilibrium with the eutectic liquid (In–22 at.% Bi) was evaluated to be $(40.4 \pm 4.0) \times 10^{-3}$ J m^{-2} using the values of Γ and ΔS_f. The experimental error in the determination of solid–liquid interface energy is the sum of the experimental errors of the Gibbs–Thomson coefficient and the entropy change of fusion per unit volume. Thus, the total experimental error of the solid–liquid interfacial energy evaluation in the present work is about 10%.

A comparison of the solid–liquid interfacial energy measured in the present work with the values obtained in previous works is given in table 4. As can be seen from table 4, our experimental value of σ_{SL} is in good agreement with the values of σ_{SL} obtained in previous works.

3.4. Grain boundary energy

If the grains on either side of the interface are the same phase, then the grain boundary energy can be expressed by

$$\sigma_{gb} = 2\sigma_{SL} \cos\theta, \tag{27}$$

where $\theta = \frac{\theta_A + \theta_B}{2}$ is the angle that the solid–liquid interfaces make with the y axis as shown in figure 1. The angles θ_A and θ_B were obtained from the cusp coordinates, x, y, using a Taylor expansion for parts at the base of the groove. According to equation (27), the value of σ_{gb} should be smaller or equal to twice that of the solid–liquid interface energy, i.e. $\sigma_{gb} \leqslant 2\sigma_{SL}$.

The value of the grain boundary energy for the solid In solution phase (In–12.4 at.% Bi) was found to be $(79.0 \pm 8.7) \times 10^{-3}$ J m^{-2} using the values of the σ_{SL} and θ into equation (27). The estimated error in determination of the θ angles was found to be 1%. Thus the total experimental error in the resulting grain boundary energy is about 11%.

4. Conclusion

The radial heat flow apparatus was used to observe the equilibrated grain boundary groove shapes for alloys having a lower melting temperature (smaller then 100 °C) and the solid In solution (In–12.4 at.% Bi) grains were equilibrated with In Bi eutectic liquid (In–22 at.% Bi) at 72 °C. The Gibbs–Thomson coefficient and the solid–liquid interfacial energy of the solid In solution in equilibrium with In–22 at.% Bi eutectic liquid have been determined from

the equilibrated grain boundary groove shapes using a numerical model. The grain boundary energy of the solid In solution phase has been calculated by considering a force balance at the grain boundary grooves. The thermal conductivities of the In–Bi eutectic liquid phase and the solid In solution phase and their ratio at the eutectic temperature have also been measured using radial heat flow apparatus and Bridgman-type growth apparatus.

Acknowledgments

This research was supported financially by the Scientific and Technical Research Council of Turkey (TÜBİTAK under contract no. 105T481). The authors are grateful to the Scientific and Technical Research Council of Turkey, TUBİTAK, for their financial supports.

References

[1] Eustathopoulos N, Nicholas M G and Drevet B 1999 *Wettability at High Temperatures* (Oxford: Pergamon)
[2] Martin J W, Doherty R D and Cantor B 1976 *Stability of Microstructure in Metallic Systems* (Cambridge: Cambridge University Press)
[3] Turnbull D 1950 *J. Appl. Phys.* **21** 1022
[4] Jones D R H 1974 *J. Mater. Sci.* **9** 1
[5] Eustathopoulos N 1983 *Int. Met. Rev.* **28** 189
[6] Bolling G F and Tiller W A 1960 *J. Appl. Phys.* **31** 1345
[7] Jones D R H and Chadwick G A 1970 *Phil. Mag.* **22** 291
[8] Nash G E and Glicksman M E 1971 *Phil. Mag.* **24** 577
[9] Jones D R H and Chadwick G A 1971 *J. Cryst. Growth* **11** 260
[10] Jones D R H 1978 *Phil. Mag.* **27** 569
[11] Schaefer R J, Glicksman M E and Ayers J D 1975 *Phil. Mag.* **32** 725
[12] Hardy S C 1977 *Phil. Mag.* **35** 471
[13] Singh N B and Glicksman M E 1989 *J. Cryst. Growth* **98** 573
[14] Hoyt J J, Asta M, Haxhimali T, Karma A, Napolitano R E and Trivedi R 2004 *MRS Bull.* **29** 935
[15] Gündüz M and Hunt J D 1985 *Acta Metall.* **33** 1651
[16] Gündüz M and Hunt J D 1989 *Acta Metall.* **37** 1839
[17] Maraşlı N and Hunt J D 1996 *Acta Mater.* **44** 1085
[18] Keşlioğlu K and Maraşlı N 2004 *Mater. Sci. Eng.* A **369** 294
[19] Keşlioğlu K and Maraşlı N 2004 *Metall. Mater. Trans.* A **35A** 3665
[20] Erol M, Keşlioğlu K and Maraşlı N 2007 *J. Phys.: Condens. Matter* **19** 176003:14pp
[21] Bayender B, Maraşlı N, Çadırlı E, Şişman H and Gündüz M 1998 *J. Cryst. Growth* **194** 119
[22] Hunt J D, Jackson K A and Brown H 1966 *Rev. Sci. Instrum.* **37** 805
[23] Maraşlı N, Keşlioğlu K and Arslan B 2003 *J. Cryst. Growth* **247** 613
[24] Ocak Y, Akbulut S, Böyük U, Erol M, Keşlioğlu K and Maraşlı N 2006 *Scr. Mater.* **55** 235
[25] Akbulut S, Ocak Y, Böyük U, Erol M, Keşlioğlu K and Maraşlı N 2007 *J. Appl. Phys.* **100** 123505
[26] Böyük U, Keşlioğlu K and Maraşlı N 2007 *J. Phys.: Condens. Matter* **19** 116202
[27] Hansen M and Anderko K 1958 *Constitutions of Binary Alloys* (New York: McGraw-Hill) p 303
[28] Touloukian Y S, Powell R W, Ho C Y and Klemens P G 1970 *Thermal Conductivity Metallic Elements and Alloys* vol 1 (New York: Plenum) pp 39–40
[29] Touloukian Y S, Powell R W, Ho C Y and Klemens P G 1970 *Thermal Conductivity Metallic Elements and Alloys* vol 1 (New York: Plenum) p 149
[30] Porter D A and Easterling K E 1991 *Phase Transformations in Metals and Alloys* (London: Van Nostrand-Reinhold) p 204
[31] McCartney D G 1981 *DPhil. Thesis* University of Oxford, UK, p 85
[32] Erol M, Keşlioğlu K, Şahingöz R and Maraşlı N 2005 *Met. Mater. Int.* **11** 421
[33] Hengli L, Lizhu S and Muyu Z J 1990 *Chem. Thermodyn.* **22** 821–6
[34] Christian J W 1975 *The Theory of Transformations in Metals and Alloys Part I* 2nd edn (Oxford: Pergamon) p 169
[35] Tassa M and Hunt J D 1976 *J. Cryst. Growth* **34** 38
[36] Waseda Y and Miller W A 1978 *Trans. Japan. Inst. Met.* **19** 546–52

[37] Skripov V P 1977 Homogeneous nucleation metals and amorphous films *Crystal Growth and Materials* ed E Kaldis and H Schell (Amsterdam: North-Holland) p 327
[38] Miedema A R and den Broeder F J A 1979 *Kolloid Z.* **70** 14–20
[39] Jones H 2002 *Mater. Lett.* **53** 364–6
[40] Digilov R M 2004 *Surf. Sci.* **555** 68–74